Polymer Chemistry

Accepted Manuscript

This is an *Accepted Manuscript*, which has been through the Royal Society of Chemistry peer review process and has been accepted for publication.

Accepted Manuscripts are published online shortly after acceptance, before technical editing, formatting and proof reading. Using this free service, authors can make their results available to the community, in citable form, before we publish the edited article. We will replace this *Accepted Manuscript* with the edited and formatted *Advance Article* as soon as it is available.

You can find more information about *Accepted Manuscripts* in the Information for Authors.

Please note that technical editing may introduce minor changes to the text and/or graphics, which may alter content. The journal's standard Terms & Conditions and the Ethical guidelines still apply. In no event shall the Royal Society of Chemistry be held responsible for any errors or omissions in this *Accepted Manuscript* or any consequences arising from the use of any information it contains.

ROYAL SOCIETY OF CHEMISTRY

www.rsc.org/polymers

Rheological Behavior and Molecular Relaxation of Polycations with Macrocounterions in Aqueous Solutions

Yilan Ye [a, b], Shangguan Yonggang [*, a], Qiang Zheng [*, a]

[a] *MOE Key Laboratory of Macromolecular Synthesis and Functionalization, Department of Polymer Science and Engineering, Zhejiang University, Hangzhou 310027, China.*

[b] *Department of Materials Science and Engineering, The Pennsylvania State University, University Park, Pennsylvania 16802.*

* *Corresponding Authors. Email address: shangguan@zju.edu.cn (Yonggang Shangguan), zhengqiang@zju.edu.cn (Qiang Zheng). Tel: +86 57187953075.*

Abstract

Counterions play significant roles in the characteristics of polyelectrolytes, whereas many problems still remain unsolved. Among most previous researches, counterions were too small to be "seen" by light scattering. In this article, we prepare macrocounterions which are single/double carboxylate ion-terminated polyethylene glycols ($M_n \approx 5000$ g/mol). Solution properties of polycations with macrocounterions are investigated through rheological, conductivity and dynamic light scattering measurement. On the basis of the scaling theory, the static and dynamic parameters of polyelectrolytes are analyzed over wide concentration ranges. In rheological measurement, a critical concentration (c^*_{mc}) has been observed. When concentration is below c^*_{mc}, the role of macrocounterions can be ignored; while above c^*_{mc}, macrocounterions determine the longest relaxation and prevent entanglement of polycations. Moreover, the same turning point exists in the dependence of

Polymer Chemistry Accepted Manuscript

conductivity and viscosity on the molar fraction of macrocounterions, which indicates that macrocounterions can't serve as brushes condensed on the polycation until their molar fraction is above the effective charge density of polyelectrolytes. In dynamic light scattering, we investigate the relaxation of polycations with macrocounterions on the length scale of electrostatic blobs, where the size of macrocounterions becomes significant. In comparison with ordinary polyelectrolytes, it is observed that both fast and slow diffusive relaxations of polycations with macrocounterions are significantly slowed down, and fast mode relaxation becomes dominant. Since no independent relaxation of macrocounterions has been observed, it is supposed that the fast mode relaxation is the coupled relaxation of polycations and macrocounterions.

Introduction

Polyelectrolytes, consisted of polyions and multiple counterions, are considered as one of the least understood condensed matters due to the complex long-range electrostatic interaction and multi-component system. In particular, counterions can influence the static structure and dynamics of polyelectrolytes dramatically.[1-5] Strong electrostatic interaction between polyions and counterions of high charge density has been observed, including counterions of multivalent ions, oppositely charged polyelectrolytes and polyzwitterions. For example, multivalent counterions can cause like-charged polyelectrolytes to condense into compact ordered states, *e.g* DNA toroids and F-actin bundles[6-8]; oppositely charged polyelectrolytes can form complexes which can be utilized in layer-by-layer assembly[9], high-performance membranes[10] and hydrogels of extremely high mechanical strength[11]; polyzwitterions

Polymer Chemistry Accepted Manuscript

exhibit anti-polyelectrolyte properties because their counterions are covalently bonded with polyions.[12, 13] In dynamic light scattering (DLS), polyelectrolytes have been observed to exhibit both fast and slow mode relaxation. Concerning the fast mode relaxation, it is supposed to be the coupling movement of the polyion with counterions.[4, 14, 15] Matsuoka *et al.*[4] found that fast mode follows the order of $Li^+ < Na^+ < Cs^+ < H^+$ which is consistent with ion mobility and hydration size, although the difference was small. For divalent counterions (Mg^{2+}), the fast mode becomes slower and the slow mode becomes faster, in comparison with the monovalent counterion (Na^+).[14]

Among researches in the past, counterions were too small to be “seen” in scattering measurements. Thus, a question arises: if the counterions are as large as visible in light scattering, how will such macrocounterions influence the conformation as well as dynamics of polyions? In this study, we prepare macrocounterions which are carboxylate ion-terminated poly(ethylene glycol) (PEG) of about 5000 g/mol. As is well-known, PEG is neutral polymer which exhibits good solubility in water[16]. Therefore, the macrocounterions are able to dissolve in water readily, as opposed to ionic surfactants which will form micelles in water. Moreover, PEG bear diverse properties such as crystallization, solubility in organic solvent[17] and good solvation of cations which is ideal for lithium ion batteries.[18, 19] Therefore, the long PEG tails of the macrocounterions could possibly endow polyelectrolytes with some novel properties. Concerning the high molecular weight of the macrocounterions, it is supposed that (i) their conformation and relaxation behaviors can be detectable; (ii)

Polymer Chemistry Accepted Manuscript

their electrophoretic mobility will be much slower than those of small counterions; and (iii) the condensed macrocounterions can be considered as self-assembled brushes on polyions. In this article, both single and double carboxylate ion-terminated PEG were prepared. On the basis of the scaling theory, we will first investigate the specific viscosity (η_{sp}), the longest relaxation time (τ) and the terminal modulus (G) of polyelectrolytes with macrocounterion over wide concentration ranges through rheological measurement. Then dependence of solution conductivity on molar fraction of macrocounterions will be investigated. In addition, diffusive relaxation of electrostatic blobs of polycations with macrocounterions in dilute solution will be investigated by DLS.

Experimental Section

1. Materials

Poly(ethylene glycol) (PEG, M_n = 4,600 g/mol) and poly(ethylene glycol) methyl ether (MPEG, M_n = 5,000 g/mol) were purchased from Aldrich, USA. Toluene (AR) and tetrahydrofuran (THF, AR) were purchased from SCRC, China and were distilled over sodium/benzophenone ketyl under a dry N_2 atmosphere prior to use. Succinic anhydride (> 95 %), 4-dimethylaminopyridine (DMAP, > 99%), triethylamine (> 99 %), methyl 2-chloropropionate (MCP, > 95%) and (3-acrylamidopropyl)trimethylammonium chloride (ATP-Cl, 74~75% in water) were purchased from TCI, Japan. *N*, *N*-dimethylformamide (DMF, AR), ammonium persulfate ($(NH_4)_2S_2O_8$, AR), sodium bisulfite ($NaHSO_3$, AR) and sodium hydroxide (NaOH, AR) were purchased from SCRC, China and were used as received. Copper (I)

Polymer Chemistry Accepted Manuscript

chloride (CuCl, > 97%) from Fluka, USA was washed with acetic acid followed by methanol to remove impurities. Tris(2-dimethylaminoethyl)amine (Me6TREN, > 99%) was purchased from Alfa Aesar, USA. Deuterium oxide (D_2O, 99.9 %) was purchased from TenglongWeibo Technology, China. Deuteriochloroform ($CDCl_3$, 99.8 %) was purchased from Cambridge Isotope Laboratories, Inc., USA. Ultrapure water with resistivity of 18.25 MΩ·cm was produced by ULUPURE water purification system, China. Strong anion exchange resins D-201 were purchased from Aladdin, China.

2. Synthesis

2.1 Synthesis of Carboxyl-Terminated MPEG (MPC)

MPEG (45.40g, 8.86 mmol) was dried by azeotropic distillation in 200 mL toluene at 135 ~ 140 ºC. The dry MPEG, succinic anhydride (1.78g 17.72 mmol), DMAP (1.08g, 8.86mmol) and triethylamine (123 μL, 0.89 mmol) were dissolved in 400 mL THF. The reaction was carried out at 20 ºC under vigorous stirring. After 72 h, the solvent was evaporated completely using a rotary evaporator. The solid residue was dissolved in ultrapure water, and the precipitates were removed through pumping filtration. Then filtrate was dialyzed in dialysis tubes (cutoff molecular weight: 3500 g/mol) against ultrapure water, until the conductivity of the emerging dialyzate is below 2 μs/cm. Finally, the dialyzed solutions were dehydrated through lyophilization. ^1H NMR ($CDCl_3$, 500 MHz): 4.20 (t, $COOCH_2$), 3.60 (m, OCH_2CH_2O), 3.33 (s, CH_3O), 2.59 (m, $OCOCH_2CH_2OCO$).

Polymer Chemistry Accepted Manuscript

2.2 Synthesis of Carboxyl-Terminated PEG (CPC)

The synthesis and purification of CPC was similar to that of MPC, with dry PEG (29.41 g, 6.31 mmol), succinic anhydride (2.52g, 25.24 mmol), DMAP (1.54g, 12.62 mmol) and triethylamine (177μL, 1.26 mmol) dissolved in 300 mL THF. ^{1}H NMR ($CDCl_3$, 500 MHz): 4.24 (t, $COOCH_2$), 3.66 (m, OCH_2CH_2O), 2.63 (m, $OCOCH_2CH_2OCO$).

2.3 Synthesis of PATP-OH

2.3.1 Free Radical Polymerization

Complete exchange of chloride ion (Cl^-) into hydroxide ion (OH^-) for monomer ATP-Cl (29.41g, 106 mmol) was conducted by utilizing excess amount of ionic exchange resin. After ion exchange, the elution (ATP-OH) was concentrated by rotary evaporation under vacuum pressure. 1 mmol $(NH_4)_2S_2O_8$ was added to 200 mL ATP-OH aqueous solution at about 0.5 mol/L. The mixture was degassed by bubbling nitrogen gas for 1 h. Then 0.1 mmol $NaHSO_3$ were added to initiate the reaction. The reaction was carried out at 25 ºC. After 20 h, the products were dialyzed in dialysis tubes (cutoff molecular weight: 14,000 g/mol) against ultrapure water, until the conductivity of the emerging dialyzate was around 2 μs/cm. Finally, the dialyzed polyelectrolyte solution (PATP-OH) was concentrated by rotary evaporation under vacuum pressure. The concentrated solution was stored in polyethylene bottles and its monomer concentration was 94.65 mmol/L calibrated by neutralization titration.

Polymer Chemistry Accepted Manuscript

2.3.2 Atom Transfer Radical Polymerization (ATRP)

In contrast to free radical polymerization mentioned above, ion exchange was conducted after ATRP synthesis to avoid precipitates of copper (I) hydroxide (CuOH) during the reaction. ATP-Cl (29.97g, 0.11 mol) was dissolved in DMF/H_2O (45 mL / 37.5 mL) with [ATP-Cl] = 1.25 mol/L. The molar ratio of the reagents was followed by [ATP-Cl]:[MCP]:[CuCl]:[Me_6TREN]=200:1:1:1. MCP (0.06 g), and Me_6TREN (0.13 g) were added into the solution. Then the mixture was degassed by three freeze-pump-thaw cycles. The reaction was initiated by addition of CuCl (0.054 g) and continued for 1 h at 20 ºC. After polymerization, the products went through ion exchange to convert Cl^- into OH^- completely. The elution was purified in the same way as products of free radical polymerization. Its monomer concentration was 50.3 mmol/L calibrated by neutralization titration.

2.4 Preparation of Polyelectrolyte with Macrocounterions

Polycations with macrocounterions were prepared by neutralization reaction of PATP-OH storage solution with certain molar fraction of MPC and CPC. The highest molar fraction of macrocounterions is 90 mol%, and the rest of counterions are hydroxide ion (OH^-) to avoid hydrolysis of carboxylate ions (COO^-). Then the concentrated solutions were diluted to a series of concentrations. The storage solution was further concentrated to prepare samples of higher concentrations. All the solutions were stored in polyethylene bottles.

Polymer Chemistry Accepted Manuscript

3. Characterization

Chemical structures of MPC and CPC were characterized by proton nuclear magnetic resonance (^{1}H NMR) spectroscopy through a 500 MHz Bruker Advance III spectrometer (Germany). The weight-average molecular weight (M_w), number-average molecular weight (M_n) and polydispersity index (M_w/M_n) of polyelectrolytes were determined by gel permeation chromatography (GPC) of Waters 515 equipped with TOSOH BIOSEP G4000SWXL (7.8 × 300 mm, Japan) as hydrophilic columns. Near-monodisperse poly(ethyleneoxide) (PEO) standards were used for calibration. The eluent was 0.1 M $NaNO_3$ aqueous solution at a flow rate of 1 mL/min at 40 ºC.

4. Rheological Measurements

An AR-G2 rheometer (TA Co., USA) was utilized for rheological measurement. Steel cone-plate geometry (40 mm diameter, 2º cone angle, gap 50 μm) was used in steady shear. Temperature was controlled at 20 ºC by a Peltier system.

5. Conductivity

Conductivity was measured by conductivity meter with conductivity cell lnlab@738, Mettler Toledo Co. The cell was calibrated using standard solutions with known conductivities. Temperature is controlled at 20 ºC by water bath.

6. Laser Light Scattering

Polymer Chemistry Accepted Manuscript

Dynamic light scattering was measured by a commercial laser light scattering spectrometer (Brookhaven Instruments Corporation, USA) equipped with a digital autocorrelator (BI-9000AT) and a He-Ne laser (λ_0 = 632.8 nm). All solutions were filtered with Millpore LCR 0.2 μm. Temperature was controlled at 20 º C and angular range for measurement was from 30 º to 150 º. CONTIN method [20] was used to analyze DLS data.

Results and Discussion

Scheme 1 shows chemical structures of polyethylene glycol (PEG), double carboxyl-terminated PEG (CPC), polyethylene glycol methyl (MPEG), carboxyl-terminated MPEG (MPC), poly((3-acrylamidopropyl)trimethylammonium hydroxide) (PATP-OH), and poly ((3-acrylamidopropyl)trimethylammonium carboxylic ion-terminated MPC) (PATP-MPC). NMR characterizations of MPC and CPC are shown in the Supporting Information SI. 1 and SI. 2. Table 1 shows the M_n, M_w and M_w/M_n of PATP-OH, (PATP_ATRP)-OH, PEG and MPEG. In particular, PATP-OH is synthesized by free radical polymerization, which presents high molecular weight while broad polydispersity. On the other hand, (PATP_ATRP)-OH is synthesized by ATRP method, which exhibits much lower molecular weight while narrower polydispersity. The degree of polymerization of (PATP_ATRP)-OH is comparable to an electrostatic blob of PATP-OH, which will be discussed later.

Polymer Chemistry Accepted Manuscript

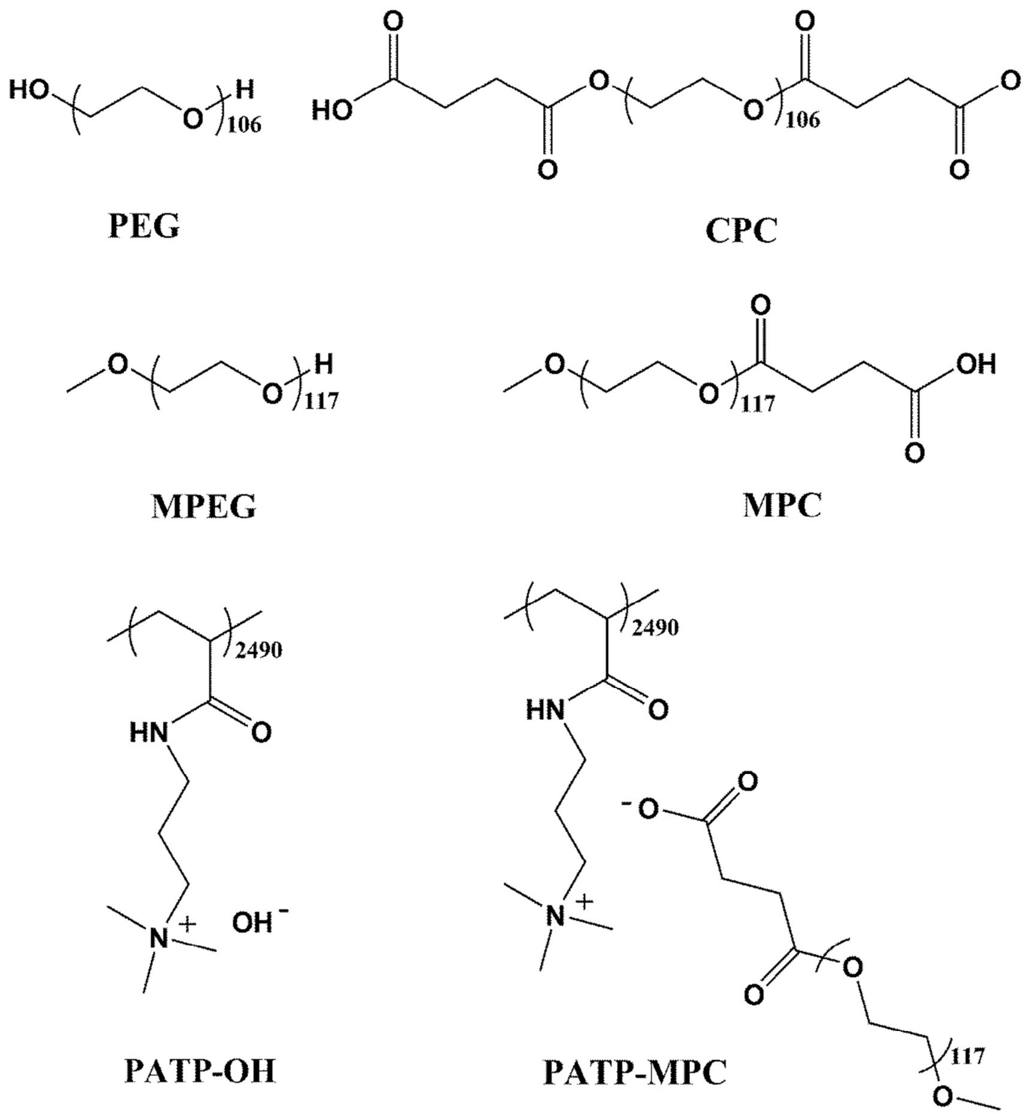

Scheme 1. Chemical structures of PEG, CPC, MPEG, MPC, PATP-OH and PATP-MPC.

Table 1. Molecular weights, polydisperity index and degree of polymerization for samples

Sample	M_n / g·mol^{-1}	M_w / g·mol^{-1}	M_w / M_n	N
PATP-OH	4.68×10^5	7.09×10^5	1.52	2490 [a]
(PATP_ATRP)-OH	5.13×10^3	5.41×10^3	1.05	27 [a]
MPC	5.22×10^3	-	-	117 [b]
CPC	4.86×10^3	-	-	106 [b]

[a] Degree of polymerization N is calculated by ratio of number-average molecular

Polymer Chemistry Accepted Manuscript

weight M_n to molecular weight of monomer.

[b] Calculated by NMR spectrum.

2. Theory Background

There are four length scales which describe the molecular structure of polyelectrolytes in solution, including Bjerrum length (l_B), electrostatic blob size (ξ_e), contour length (L) and correlation blob size (ξ).[21-23] First, Bjerrum length (l_B) is the length scale at which the electrostatic energy of two charges equals the thermal energy 1 kT,

$$l_B = e^2 / \varepsilon kT \qquad (1)$$

where e is the elementary charge, ε is the dielectric constant of solvent, k is the Boltzmann constant, and T is the absolute temperature. According to Manning theory, counterion will condense to the polyion when the distance between nearby charged monomers becomes smaller than l_B, as a result, the effective charge density f of the polyion decreases. Generally, for polyelectrolytes in water at 25 ºC, $l_B \approx 0.71$ nm, and the effective charge density $f \approx b / l_B \approx 35\%$.[23]

Secondly, an electrostatic blob size (ξ_e) is the length scale at which the electrostatic energy inside the electrostatic blob equals 1 kT,

$$(f g_e e)^2 / \varepsilon \xi_e \approx kT \qquad (2)$$

where f is the effective charge density of polyelectrolytes, ξ_e is the size of the electrostatic blob and g_e is the number of monomers inside the electrostatic blob. Inside the electrostatic blob, polyion monomers adopt self-avoiding walk, like neutral

Polymer Chemistry Accepted Manuscript

polymer in good solvent,

$$\xi_{\mathrm{e}} \approx b g_e^{3/5} \tag{3}$$

where b is the monomer size, and $b \approx 0.25$ nm for vinyl monomers in good solvent[23].

Considering the contour length (L) of a polyelectrolyte chain in dilute solution where no multi-chain interfaction exists, L is considered as an array of electrostatic blobs,

$$L \approx \xi_{\mathrm{e}} \frac{N}{g_{\mathrm{e}}} \approx bN(\frac{l_{\mathrm{B}}}{b})^{2/7} f^{4/7} \tag{4}$$

where N is the degree of polymerization of polyelectrolyte.

Lastly, the correlation blob size (ξ) describes the distance between nearby chains when concentration is over the critical overlap concentration c^*. Based on the definition, c^* is calculated by[24]

$$c^* \approx \frac{N}{L^3} \tag{5}$$

$$\xi \approx L\left(\frac{c}{c^*}\right)^{-1/2} \approx (\frac{B}{cb})^{1/2} \qquad \text{for } c > c^* \tag{6}$$

Inside the correlation blob, the polyion segments behave like they are in the dilute solution, while outside the correlation blob, electrostatic interactions are screened and the conformation of the polyion is random walk of correlation blobs.

$$R \approx \xi(N/g)^{1/2} \qquad \text{for } c > c^* \tag{7}$$

where R is the end-to-end distance of polyelectrolyte, ξ is the correlation blob size and g is the number of monomers inside the correlation blob.

Moreover, the stretching parameter B is defined as the ratio of the maximum possible contour length bN to the contour length L of the polylectrolyte,

Polymer Chemistry Accepted Manuscript

$$B \equiv bN/L \approx bN^{2/3}(c^*)^{1/3} \tag{8}$$

Replacing parameters in equations (1) ~ (6) by B, it is calculated that

$$\xi_e \approx bB^{3/2} \tag{9}$$

$$g_e \approx B^{5/2} \tag{10}$$

$$L \approx \xi_e \frac{N}{g_e} \approx Nb/B \tag{11}$$

3. Rheology

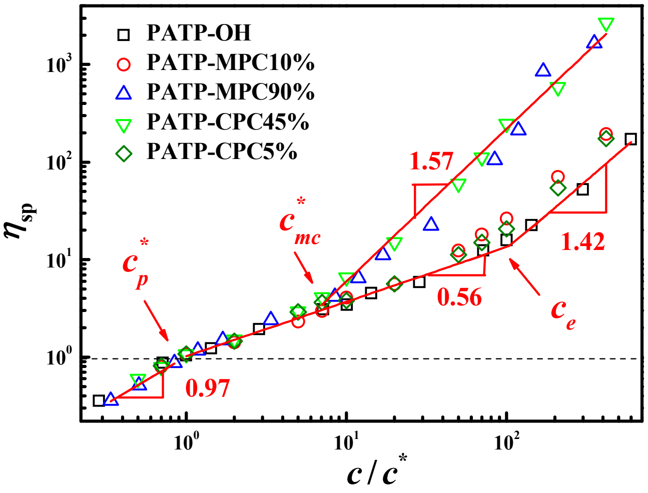

Fig. 1 Dependence of specific viscosity (η_{sp}) on normalized concentration (c/c^*) for aqueous solutions of PATP-OH, PATP-MPC10%, PATP-MPC90%, PATP-CPC5% and PATP-CPC45%. $\eta_{sp} = 1$ is guided by the line.

Fig. 1 shows dependence of specific viscosity (η_{sp}) on the normalized concentration (c/c^*) for sample PATP-OH, PATP-MPC10%, PATP-MPC90%, PATP-CPC5% and PATP-CPC45%. In terms of nomenclature, PATP refers to the polycation, while OH, MPC and CPC refer to three types of counterions respectively, including hydroxide

Polymer Chemistry Accepted Manuscript

(OH^-), single carboxylate ion-terminated MPEG (MPC^-) and double carboxylate ion-terminated PEG ($^-CPC^-$). Moreover, the number in the nomenclature means the molar fraction of macrocounterions over all the counterions, and the rest of counterions are OH^-. Note that though the molar fraction of $^-CPC^-$ is half that of MPC^-, they contain the same amount of carboxylate ion (COO^-). Concerning c^*, it is determined by the concentration which corresponds to $\eta_{sp} \approx c / c^* \approx 1$, [23] and refers to the monomer concentration. It should also be mentioned that $c / c^* \approx 400$ is the highest concentration studied for PAPT-MPC90% and PATP-CPC45% due to the maximum solubility of polyethylene in water at 20 ºC. In Fig. 1, η_{sp} of all the samples are well overlapped when $c/c^* < 7$, whereas η_{sp} of PATP-MPC90%, PATP-CPC45% deviate and become another group at higher concentration. Concerning the ordinary polyelectrolyte PATP-OH, it shows $\eta_{sp} \sim c^{0.97}$, $\eta_{sp} \sim c^{0.56}$ and $\eta_{sp} \sim c^{1.42}$ as concentration increases, which is in agreement with the theoretical scaling relation for dilute, semidilute unentangled and entangled solutions respectively.[21] In particular, entanglement of PATP-OH occurs at concentration $c/c^* \approx 100$. The η_{sp} of PATP-MPC10% and PATP-CPC5% are close to those of PATP-OH, but entanglement occurs at lower concentration and η_{sp} becomes slightly larger than that of PATP-OH in entangled solution. It is possibly that the small amounts of macrocounterions promote entanglement of the polycations. In contrast to PATP-OH, PATP-MPC10% and PATP-CPC5%, PATP-MPC90% and PATP-CPC45% exhibit $\eta_{sp} \sim c^{1.57}$ when $c/c^* > 7$. Though the scaling exponent 1.57 resembles that for entangled polyelectrolytes, it does not mean that PATP-MPC90% and PATP-CPC45% have entangled. The static

Polymer Chemistry Accepted Manuscript

structure and dynamics of polycations with macrocounterions will be analyzed on the basis of the scaling theory[21-23].

Considering the fact that all the samples present similar η_{sp} when $c/c^* < 7$, it means that the effect of macrocounterions can be ignored within this concentration region. Therefore, it is believed that the long-range electrostatic interaction is dominant, and the scaling approach to describe the conformation and dynamics of ordinary polyelectrolytes can still be applicable to polycations with macrocounterions for $c/c^* < 7$. For instance, the contour length of polycations with macrocounterions can also be described as an array of electrostatic blobs in dilute solution and the polycations can be considered as random walk of correlation blobs when $1 < c/c^* < 7$. Table 2 summarizes the static molecular parameters including the size (ξ_e) and number of monomers (g_e) of electrostatic blob, stretching parameter (B) and contour length (L) for PATP-OH, PATP-MPC10%, PATP-CPC5%, PATP-MPC90% and PATP-CPC45%, calculated by equation (7) ~ (10). In Table 2, stretching ratio B is 3.4 ~ 3.8, which indicates highly stretched conformation due to high charge density of the polycations. However, the slight difference in c^* of all the samples still needs further investigation. Scheme 2 (a) ~ (c) illustrate electrostatic blobs of PATP-OH, PATP-MPC90% and PATP-CPC45% respectively in accompanying with their counterions in dilute solution. In Scheme 2 (a), the electrostatic blob of $\xi_e \approx 1.4$ nm and $g_e \approx 20$ is at the center, closely surrounded by condensed counterions (OH^-), and the uncondensed OH^- are relatively far away from the center. In Scheme 2 (b) the electrostatic blob of PATP-MPC90% of $\xi_e \approx 1.4$ nm and $g_e \approx 18$ is surrounded by brush-like

Polymer Chemistry Accepted Manuscript

macrocounterions (MPC$^-$), with condensed and uncondensed MPC$^-$ at inner and outer space respectively. It is estimated that the end-to-end distance of MPC$^-$ is $R_{\mathrm{mc}} \approx \sqrt{C_{\infty} N b^2} \approx 7$ nm, where $N = 117$, $b = 0.25$ nm and $C_{\infty} = 6.7$ are respectively degree of polymerization of MPC, monomer size and characteristic ratio for poly(ethylene oxide) in Θ solvent.[24] Therefore, R_{mc} is about 5 times ξ_{e}, and the radius of the shell around the electrostatic blob is even larger due to existence of uncondensed MPC$^-$. In Scheme 2 (c), for electrostatic blob of PATP-CPC45% of $\xi_{\mathrm{e}} \approx 1.9$ nm and $g_{\mathrm{e}} \approx 28$, there are condensed $^-$CPC$^-$ close to electrostatic blobs and uncondensed $^-$CPC$^-$ at the outer space of the electrostatic blobs. Noted that amount of $^-$CPC$^-$ is half that of MPC$^-$ because of their double carboxylate ions. Moreover, concerning double carboxylate ions of $^-$CPC$^-$, only intra-chain condensation will take place in dilute solution. Scheme 2 (d) shows the single chain conformation of PATP-MPC90%. MPC$^-$ could serve as brushes which increase the rigidity of the polycation. Though the size of MPC$^-$ (R_{mc}) is about 5 times the ξ_{e}, the contour length of the polycation is much larger than R_{mc}, with the ratio $R_{\mathrm{mc}}/L \approx 7\,\mathrm{nm}/194\,\mathrm{nm} \approx 4\%$. In terms of topological structure, polycations with macrocounterions can be analogous to polymacromonomers, which contains high density of combs.[25, 26]

Table 2. Molecular parameters of polyelectrolytes

Sample	c^* / mmol·L^{-1}	ξ_e / nm	g_e	B	L / nm
PATP-OH	0.66	1.5	20	3.4	190
PATP-MPC90%	0.56	1.4	18	3.2	194
PATP-CPC45%	0.95	1.9	28	3.8	169
PATP-MPC10%	0.95	1.9	28	3.8	169
PATP-CPC5%	0.95	1.9	28	3.8	169

Polymer Chemistry Accepted Manuscript

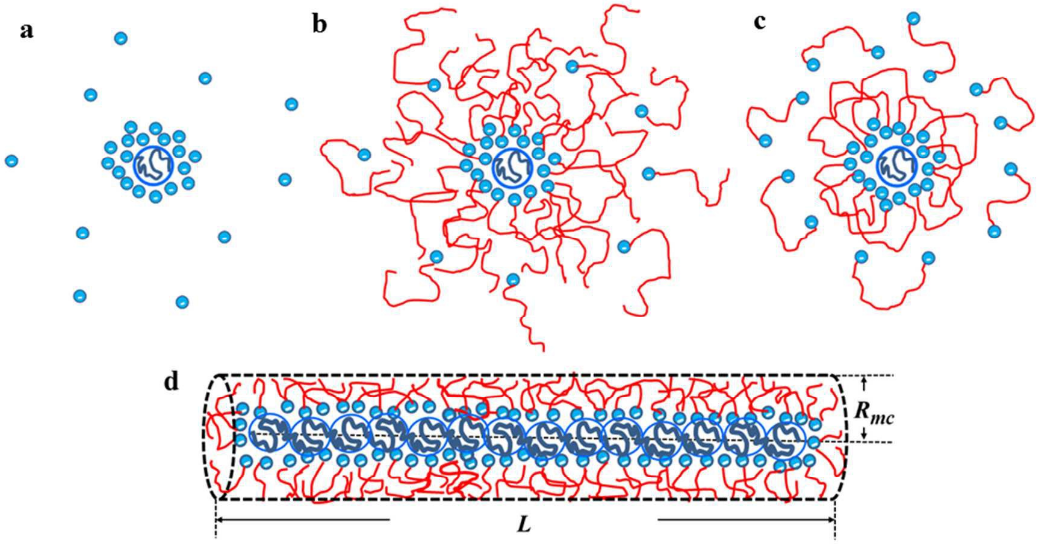

Scheme 2. Illustrations of electrostatic blobs and counterions of (a) PATP-OH, (b) PATP-MPC90% and (c) PATP-CPC45%, and single chain conformation of (d) PATP-MPC90% in dilute solution. The large blue circle at the center represents an electrostatic blob, the small blue circles around the electrostatic blob represent OH$^-$, and the red tails with single/double blue circles at the ends represent MPC$^-$/$^-$CPC$^-$.

Polymer Chemistry Accepted Manuscript

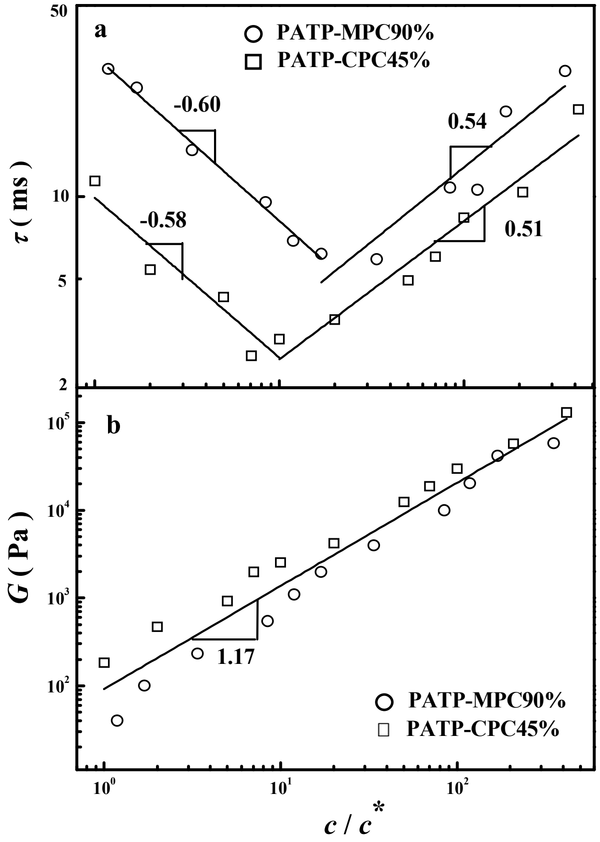

Fig. 2 Dependence of the longest relaxation time (τ) and terminal modulus (G) on the normalized concentration (c/c^*) for sample PATP-MPC90% and PATP-CPC45%.

Fig. 2 shows dependence of the longest relaxation time (τ) and the terminal modulus (G) on the normalized concentration (c/c^*) for sample PATP-MPC90% and PATP-CPC45%. Here, τ and G refer to the relaxation time and modulus on length scale of the whole chain, where τ is obtained by fitting the Carreau model and G is determined by $G = \eta / \tau$.[23] Fig. 2(b) shows that $G \sim c^{1.17}$, which agrees with the scaling relation of unentangled polymers[22]. In analogy to polymacromonomers whose dense brushes prevent entanglement of the linear backbone[25], the dense brush-like macrocounterions will also increase the rigidity of the polycations and prevent them

Polymer Chemistry Accepted Manuscript

from entanglement. In Fig. 2(a), τ presents two slopes as concentration increases. At beginning, the slopes of PATP-MPC90% and PATP-CPC45% are -0.6 and -0.58 respectively, close to the scaling exponent of ordinary polyelectrolytes (-0.5) in semidilute unentangled solutions. As c/c^* further increase to 20 and 10 for PATP-MPC90% and PATP-CPC45% respectively, slopes of τ change to 0.54 and 0.51 respectively. In comparison to the scaling relation of relaxation of entangled polyelectrolytes ($\tau \sim c^0$), the unique scaling relation of PATP-MPC90% and PATP-CPC45% ($\tau \sim c^{0.5}$) indicates characteristic dynamics of polycations with macrocounterions rather than entanglement.

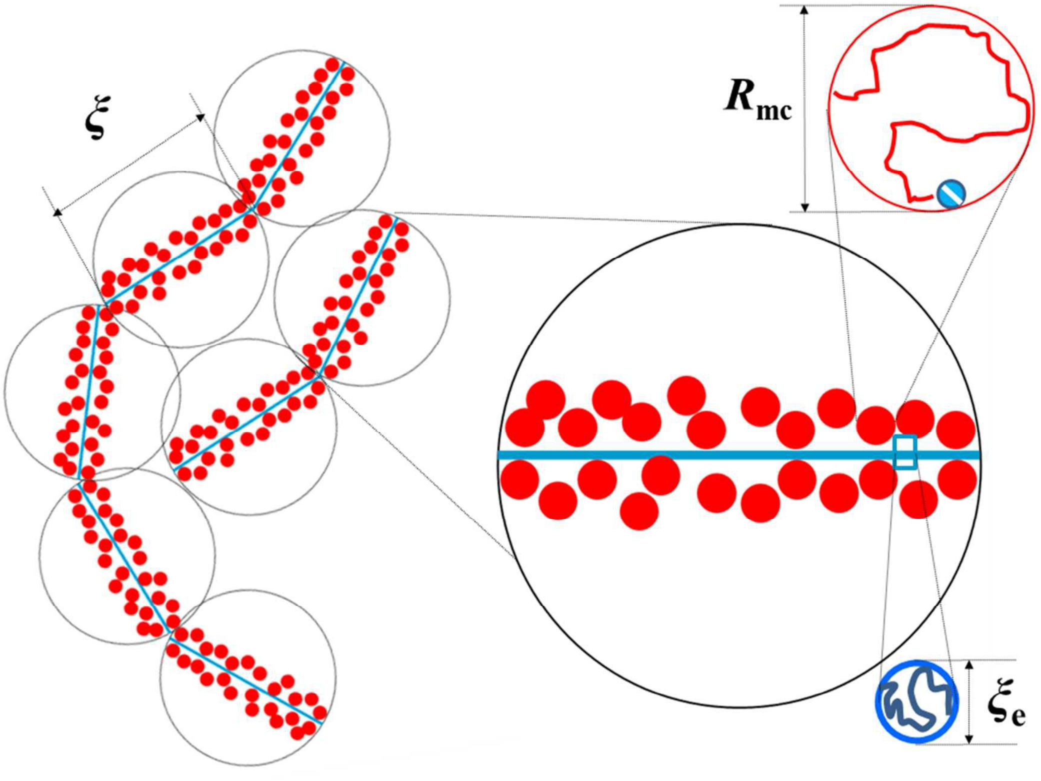

Scheme 3. Illustration of correlation blobs of PATP-MPC90%.

Polymer Chemistry Accepted Manuscript

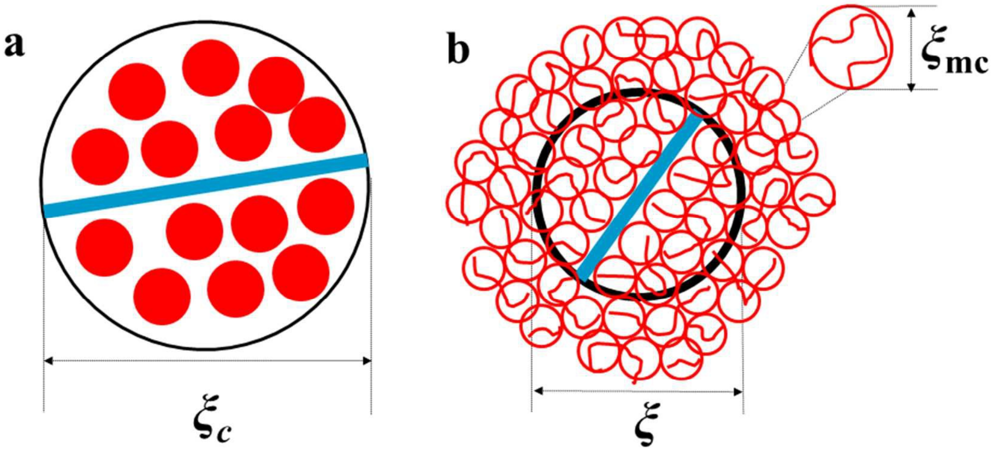

Scheme 4. Illustration of a correlation blob of PATP-MPC90% at (a) critical concentration c_c and (b) above c_c.

Scheme 3 illustrates the random walk of correlation blobs of PATP-MPC90% when $c/c^* > 1$, on the basis that the electrostatic interaction is dominant on long length scale and therefore correlation blobs predicted for ordinary polyelectrolytes are applicable to polycations with macrocounterions. In analogy to comb polyelectrolytes, Papagiannopoulos and his coworkers[27, 28] confirmed that the correlation length of comb polyelectrolytes is independent of comb architecture through small angle X-ray scattering (SAXS) measurement. But it should be noted that for comb polyelectrolytes above c^*, their backbones and side chains are polyelectrolytes consisted of the same type of correlation blobs, while for polycations with macrocounterions, each correaltion blob contains polycations surrounded by macrocoutnerions with neutral tails. In Scheme 3, the left part shows random walk of correlation blobs. Each blob is of size ξ and contains g monomers of polycation as well as g macrocounterions (MPC$^-$). The conformation of polycation inside the correlation blob, represented by

Polymer Chemistry Accepted Manuscript

Polymer Chemistry Accepted Manuscript

thick blue line, is an array of electrostatic blobs of size ξ_e, and MPC$^-$ are represented by red circles whose size is R_{mc}. When concentration is slightly above c^*, the size of the correlation blob ξ is close to the contour length (L) of the polycation and $\xi >> R_{mc}$, similar to Scheme 2(d). Therefore, the effect of macrocounterions on the relaxation time of correlation blob (τ_{blob}) can be ignored, and τ_{blob} follows Zimm mode as ordinary polyelectrolytes,

$$\tau_{\mathrm{blob}} \approx \eta_s \xi^3 / kT \tag{12}$$

where η_s is solvent viscosity. As concentration further increases, ξ decreases as $\xi \sim c^{-1/2}$ and the longest relaxation time τ also decreases as $\tau \sim c^{-1/2}$, as ordinary polyelectrolytes do[22]. However, once concentration reaches a critical value c_c, it is supposed that the role of macrocounterions becomes dominant. Scheme 4(a) shows a correlation blob at c_c, where g_{c} macrocounterions of volume R_{mc}^3 fill the space of the critical correlation blob ξ_{c}^3, namely

$$\xi_{\mathrm{c}}^3 \approx g_{\mathrm{c}} R_{\mathrm{mc}}^3 \tag{13}$$

Concerning the definition of critical overlap concentration, c_c in fact equals the critical overlap concentration of macrocounterions (c_{mc}^*). As shown in Scheme 4(b), when $c > c_c$, macrocounterions become overlapped and each macrocounterion is random walk of their own correlation blobs of size ξ_{mc}, represented by red circles. Inside ξ_{mc}, there are g_{mc} macrocounterion monomers which relax in Zimm mode, so the relaxation time of each blob ($\tau_{\mathrm{blob\_mc}}$) is

$$\tau_{\mathrm{blob\_mc}} \approx \eta_s \xi_{\mathrm{mc}}^3 / kT \tag{14}$$

The correlation blob of polycations is represented by the thick black circle of size ξ.

Since macrocounterions serve as thick shells around the polycation, the polycation cannot relax until the macrocounterions around the polycation have relaxed. Therefore, the relaxation time of correlation blob of polycations (τ_{blob}) is determined by Rouse mode relaxation of multiple correlation blobs of macrocounterions. If one macrocounterion contains n monomers, each correlation blob of polycations contains $(n/g_{\text{mc}})g$ correlation blobs of macrocounterions, so

$$\tau_{\text{blob}} \approx \tau_{\text{blob\_mc}}\left(\frac{ng}{g_{\text{mc}}}\right)^2 \qquad (15)$$

Concerning the relaxation of the whole chain of polycation with macrocounterions (τ_{chain}), it is Rouse mode relaxation of N/g correlation blobs of polycation,

$$\tau_{\text{chain}} \approx \tau_{\text{blob}}\left(\frac{N}{g}\right)^2 \approx \tau_{\text{blob\_mc}}\left(\frac{Nn}{g_{\text{mc}}}\right)^2 \sim N^2 n^2 c^{(2-3\upsilon)/(3\upsilon-1)} \qquad (16)$$

where for neutral polymers, $v = 0.5$ in Θ solvent, and $v = 0.588$ in good solvent, while for polyelectrolytes, $v = 1$.[22] Since the long tails of macrocounterions are neutral polyethylene glycol, equation (16) is calculated to be $\tau_{\text{chain}} \sim c^1$ in Θ solvent and $\tau_{\text{chain}} \sim c^{0.31}$ in good solvent. Therefore, the scaling exponent for relaxation time of polycations with macrocounterions will be 0.31 ~ 1, dependent on the solvent quality for macrocounterions. Experimentally, the scaling relation is $\tau_{\text{chain}} \sim c^{0.5}$, which is within the theoretical prediction. In essence, the relaxation time of polycations with macrocounterions is determined by relaxation of its macrocounterions in semidilute unentangled solution.

Next we will compare the calculated c_c with the experimental result. The c^*_{mc} of MPEG and PEG is measured to be about 14 mmol/L, determined by concentration corresponding to $\eta_{\text{sp}} \approx 1$. Therefore, the normalized critical concentration c_c/c^* of

Polymer Chemistry Accepted Manuscript

PATP-MPC90% is predicted to be $c_{\mathrm{c}}/c^{*} \approx c_{\mathrm{mc}}^{*}/c^{*} \approx 25$, which is close to the experimental turning point at $c_{\mathrm{c}}/c^{*} = 20$. For PATP-CPC45%, since the ratio of monomers of polycation to CPC is 2:1, $c_{\mathrm{c}} \approx 2c_{\mathrm{mc}}^{*}$, then $c_{\mathrm{c}}/c^{*} \approx 2c_{\mathrm{mc}}^{*}/c^{*} \approx 29$, which is three times the experimental result ($c_{\mathrm{c}}/c^{*} = 10$). The difference between the theoretical calculation and the experimental result of c_{c} for PATP-CPC45% may be attributed to more complex states of $^{-}$CPC^{-} which bears double carboxylate ions. At low concentration, $^{-}$CPC^{-} will adopt loop conformation on single chain; as concentration increases, $^{-}$CPC^{-} may also adopt bridge conformation coupling different chains. Both loop and bridge conformation of $^{-}$CPC^{-} could influence the relaxation of the polycations. Research on PATP-CPC45% is under further investigation.

In comparison with $\eta \sim c^{0.5}$ for unentangled ordinary polyelectrolytes, $\eta \sim c^{1.5}$ for polycations with macrocounterions is mainly contributed by long relaxation time τ while terminal modulus G is similar to those of ordinary linear polyelectrolytes. This phenomenon is similar to the comb polyelectrolytes such as aggrecan, whose side combs do not contribute appreciably to the modulus, instead they contribute to energy dissipation in a range of naturally occurring shock absorbing tissues. [29]

In addition, it is worth to mention that the viscosity of polycations with macrocounterions is significantly higher than that of solution mixtures of PATP-OH and MPEG (or PEG) at comparable concentrations (see Supporting Information SI. 3). Therefore, it is believed that the high viscosity of polycations with macrocounterions is not merely attributed to the addition of large amount of MPEG (or PEG), but more importantly, it is due to the characteristic relaxation of macrocounterions around the

Polymer Chemistry Accepted Manuscript

polycations.

4. Conductivity

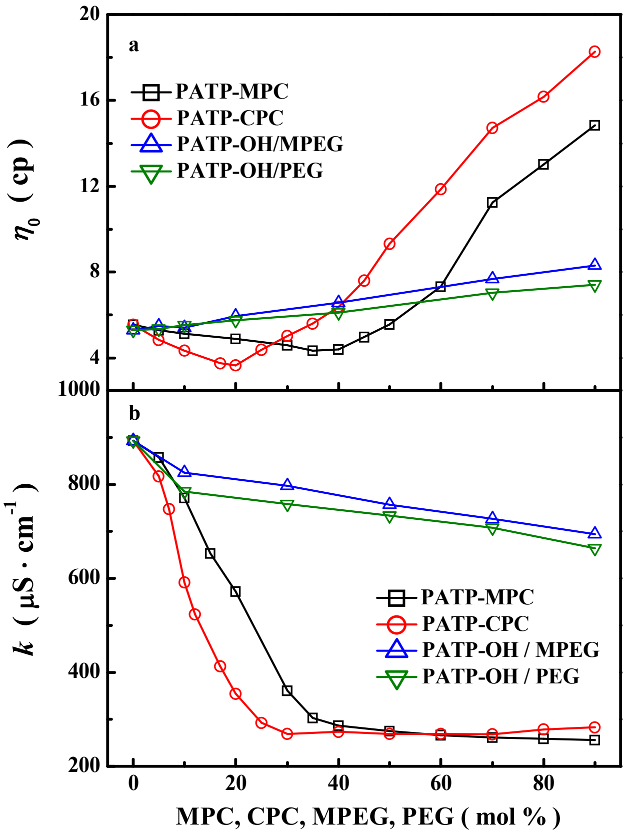

Fig. 3 (a) Dependence of zero-shear viscosity (η_0) and (b) conductivity (κ) on molar fraction of MPC, CPC, MPEG and PEG for aqueous solution of PATP-MPC, PATP-CPC, PATP-OH/MPEG and PATP-OH/PEG at 9 mmol/L at 20 ºC.

Fig. 3 shows dependences of (a) zero-shear viscosity η_0 and (b) conductivity κ on the molar fraction of MPC, CPC, MPEG and PEG for aqueous solutions of PATP-MPC, PATP-CPC, PATP-OH/MPEG and PATP-OH/PEG at 9 mmol/L at 20 ºC. In particular, PATP-OH/MPEG (or PATP-OH/PEG) is the solution mixtures of PATP-OH with various molar fraction of MPEG (or PEG). For PATP-OH/MPEG and PATP-OH/PEG, their η_0 increases while κ decreases as the molar fraction of MPEG

Polymer Chemistry Accepted Manuscript

Polymer Chemistry Accepted Manuscript

and PEG increases. The conductivity of PATP-OH/MPEG (or PATP-OH/PEG) is contributed by both polycation (κ_+) and OH$^-$ (κ_-),

$$\kappa = \kappa_+ + \kappa_- = c_{p^+}\lambda_{p^+} + c_{\mathrm{OH}^-}\lambda_{\mathrm{OH}^-} = (\lambda_{p^+} + \lambda_{\mathrm{OH}^-})c_{p^+} \quad (17)$$

where λ_{p^+} and λ_{OH^-} are the specific conductance of the polycation and OH$^-$ respectively, c_{p^+} and c_{OH^-} are the concentrations of dissociated monomers of polycations and dissociated OH$^-$ respectively and $c_{p^+} = c_{\mathrm{OH}^-}$.[30] Moreover, the specific conductance is related to ionic mobility (u),

$$\lambda_{\mathrm{OH}^-} = N_{\mathrm{A}} e u_{\mathrm{OH}^-} \quad (18)$$

$$\lambda_{p^+} = N_{\mathrm{A}} N e u_{p^+} \quad (19)$$

where u_{p^+} and u_{OH^-} are ionic mobility of the polycation and OH$^-$ respectively, N_{A} is Avogadro's number, e is the elementary charge, N is the number of monomers per polycation. Furthermore, both u_{p^+} and u_{OH^-} are inversely proportional to solvent viscosity (η_s).[30] As MPEG (or PEG) are added into PATP-OH solution, they contribute to solution viscosity, which can be considered as increase of solvent viscosity (η_s). Therefore, u_{p^+} and u_{OH^-} decrease as η_s increases. Correspondingly, λ_{p^+} and λ_{OH^-} decrease, and solution conductivity κ falls. Concerning PATP-MPC and PATP-CPC solutions, as MPC or CPC are added to PATP-OH, neutralization reaction takes place where certain amount of OH$^-$ is replaced by MPC$^-$ or $^-$CPC$^-$. It is observed that κ first decrease rapidly and then keep constant, while η_0 first decrease slightly and then increase significantly. The turning points of κ and η_0 are almost the same, namely 40 and 20 mol% for PATP-MPC and PATP-CPC respectively. The conductivity of PATP-MPC solution can be written as $\kappa = \kappa_+ + \kappa_- =$

$$c_{p^+}\lambda_{p^+} + c_{\mathrm{OH}^-}\lambda_{\mathrm{OH}^-} + c_{\mathrm{MPC}^-}\lambda_{\mathrm{MPC}^-} \qquad (20)$$

where λ_{p^+}, λ_{OH^-} and λ_{MPC^-} are the specific conductance of the polycation, OH^- and MPC^- respectively, c_{p^+}, c_{OH^-}, and $c_{\mathrm{MP}C^-}$ are concentrations of dissociated monomers of polycations, dissociated OH^- and dissociated MPC^- respectively. The concentration of cations equals that of anions due to electrostatic neutrality, and it is assumed that the effective charge density of polyelectrolytes keeps constant, so

$$c_{p^+} = c_{\mathrm{OH}^-} + c_{\mathrm{MP}C^-} = \text{constant} \qquad (21)$$

Therefore, equation (20) can be written as

$$\kappa = (\lambda_{p^+} + \lambda_{\mathrm{OH}^-})c_{p^+} + (\lambda_{\mathrm{MPC}^-} - \lambda_{\mathrm{OH}^-})c_{\mathrm{MP}C^-} \qquad (22)$$

where λ_{p^+}, λ_{OH^-} and λ_{MPC^-} are assumed to be constants since there is no change in solvent viscosity η_s or temperature. Moreover, $\lambda_{\mathrm{MPC}^-} - \lambda_{\mathrm{OH}^-} < 0$ since OH^- exhibit higher ionic mobility due to smaller hydrodynamic radius in comparison with MPC^-. Therefore, κ changes with $c_{\mathrm{MP}C^-}$ in equation (22). Comparing equation (17) and (22), it is understandable that κ of PATP-MPC is lower than that of PATP-OH/MPEG or PATP-OH/PEG due to replacement of OH^- by MPC^-. This can also be verified by the result that the concentration of OH^- decreases in the same trend as κ does when CPC are added to PATP-OH (see Supporting Information SI.4). As κ becomes constant when more MPC^- are added, it indicates that $c_{\mathrm{MP}C^-}$ becomes constant. This is attributed to condensation of MPC^- which makes no contribution to conductivity. Therefore, the turning point of κ indicates the effective charge density of polyelectrolytes, which is about 40 mol% for both PATP-MPC and PATP-CPC. This value is close to the prediction of Manning theory for polyelectrolytes in aqueous

Polymer Chemistry Accepted Manuscript

solution (35 %). Concerning $\eta_{0,}$ the increasing η_0 above 40 mol% (20 mol%) for PATP-MPC (PATP-CPC) can be ascribed to the condensed macrocounterions which serve as dense brushes. However, it is unclear why η_0 decreases with MPC$^-$ or $^-$CPC$^-$ below the turning point? Considering the long polyethylene glycol (PEG) tails of macrocounterions ($M_n \approx 5000$), the local dielectric constant ε is assumed to decrease due to much lower ε of PEG in comparison to water. As local dielectric constant decreases, the Coulomb's force between the macrocounterions and the polycations can be enhanced. The stronger electrostatic correlation between the free macrocounterions and the polycations will result in less electrostatic repulsion among nearby monomers of polycations and thus less stretched conformation. As molar fraction of macrocounterions increases (but still below the turning point), the conformation of polycations is more collapsed and the viscosity decreases. When the molar fraction of macrocounterions is above the turning point, condensed macrocounterions can serve as brushes on the polycations, which may compensate the less stretched conformation and even stretch the polycations due to increased molecular rigidity.

Moreover, the condensed macrocounterions are removable when NaCl is added to the solution, where Cl$^-$ can replace macrocounterions. As a result, viscosities of PATP-MPC90%, PATP-CPC45% and PATP-OH become similar to one another (see Supporting Information SI . 5).

Polymer Chemistry Accepted Manuscript

5. Dynamic Light Scattering

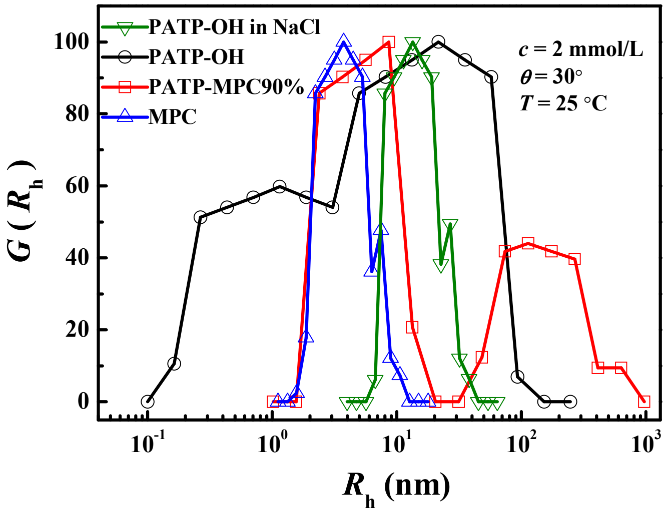

Fig 4. Distribution of hydrodynamic radius (R_h) of 2 mmol/L MPC, (PATP_ATRP)-OH, (PATP_ATRP)-MPC90% and (PATP_ATRP)-OH in the presence of 10 mmol/L NaCl at angle of 30 º and at temperature of 20 ºC.

On the basis of the static parameters of electrostatic blobs calculated in Table 2 and described in Scheme 2(a) and (b), we investigate the diffusive relaxation on length scales of electrostatic blobs by using polyelectrolytes synthesized by ATRP. The degree of polymerization of (PATP_ATRP)-OH is comparable to the number of monomers of an electrostatic blob shown in Table 2. Moreover, though the molecular weight of samples synthesized by ATRP is much lower than that of samples synthesized by free radical polymerization, (PATP_ATRP)-MPC90% still exhibit higher viscosity compared with (PATP_ATRP)-OH (see Supporting Information SI. 6). Fig. 4 shows the distribution of hydrodynamics radius (R_h) of 2mmol/L MPC, (PATP_ATRP)-OH, (PATP_ATRP)-OH in the presence of 10 mmol/L NaCl, and (PATP_ATRP)-MPC90% at angle of 30 º and at temperature of 20 ºC. The

Polymer Chemistry Accepted Manuscript

concentrations are below the c^* of (PATP_ATRP)-OH and (PATP_ATRP)-MPC90%. It is observed that R_h of MPC is 3.7 nm. As to (PATP_ATRP)-OH, two peaks of R_h are observed, which are centered at 1.1 and 21.5 nm respectively. In general, the smaller size indicates coupled diffusive motion of polycations and OH^-, while the large size indicates inter-chain interaction at the long length scale. When 10 mmol/L NaCl is added to (PATP_ATRP)-OH, the long-range electrostatic interaction has been screened. As a result, a single peak at 13.4 nm is observed which resembles its neutral counterpart. Interestingly, R_h of (PATP_ATRP)-OH with added salt is about 4 times that of MPC, though their static size ξ_e is calculated to be smaller than that of MPC. This may be attributed to the fact that large amount of charged groups of (PATP_ATRP)-OH are highly hydrated, which could contribute to stronger hydrodynamic interaction and leads to larger R_h. For (PATP_ATRP)-MPC90%, it shows two peaks of R_h, which are centered at 8.6 and 113.4 nm respectively, where the slow and fast modes become 8 and 5 times larger than those of (PATP_ATRP)-OH respectively.

Polymer Chemistry Accepted Manuscript

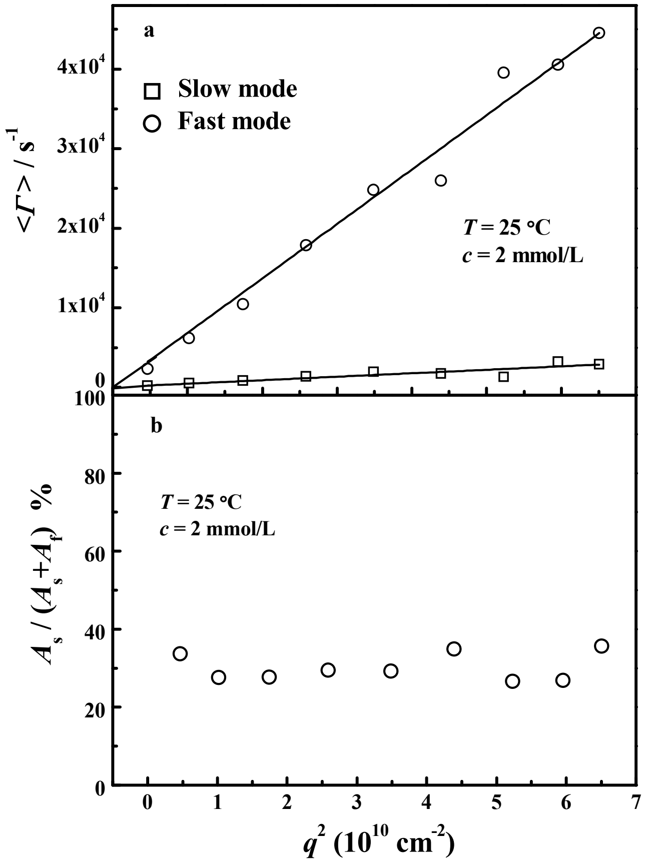

Fig 5. Scattering vector (q) dependence of (a) average characteristic line widths (Γ) and (b) intensity contribution of slow relaxation mode ($A_s/(A_s+A_f)$) for sample (PATP_ATRP)-MPC90% at 2 mmol/L and 20 ºC. Note that $A_s + A_f = 1$.The angle range is from 30~150 º.

In dynamic light scattering, the intensity autocorrelation function $<I(t)I(t+\tau)>$ can be related to the normalized electric-field autocorrelation function $|g_1(q,\tau)| = \exp(-\Gamma\tau)$, where Γ is characteristic line width. For diffusive motion, $\Gamma = Dq^2$, where D and q are diffusion coefficient and scattering vector respectively. When $g^{(1)}(q,\tau)$ contains two distinguishable relaxation modes, it can be analyzed using a combination of two exponential functions,

$$|g^{(1)}(q,t)| = A_f \exp\left(-\frac{t}{\tau_f}\right) + A_s \exp\left(-\frac{t}{\tau_s}\right) \qquad (24)$$

where A_f and A_s are intensity contributions of the fast and slow modes respectively.[31]

Polymer Chemistry Accepted Manuscript

Note that $A_s + A_f = 1$. Fig. 5 shows scattering vector (q) dependence of (a) average characteristic line widths (Γ) and (b) intensity contribution of slow relaxation mode ($A_s/(A_s+A_f)$) for sample PATP-MPC90% at 2 mmol/L and at angles from 30 º to 150 º. Fig. 5(a) shows that both slow and fast modes are diffusive motions because Γ are linear functions of q^2 passing through the origin.[31] The slopes of Γ vs q^2 lead to the fast and slow diffusion coefficient respectively, and $D_f = 6.84\times10^{-7}$ cm^2 s^{-1}, $D_s = 4.37\times10^{-8}$ cm^2 s^{-1}. The diffusion coefficients of MPC, PATP-OH in NaCl, (PATP_ATRP)-OH and (PATP_ATRP)-MPC90% are summarized in Table 3. Since the relaxation of neutral MPC can be detected by dynamic light scattering, it is possible that the independent diffusion of MPC$^-$ ($D_{MPC}{}^-$) can be observed. However, only two relaxation modes are observed. Therefore, it is supposed that the motion of MPC$^-$ is no longer independent but coupled with the polycation, which is reflected by D_f. Moreover, both D_f and D_s slowed down in comparison to (PATP_ATRP)-OH, which may be attributed to the topological constrains of multiple macrocounterions on the diffusion of polycations. Fig 5(b) shows that the intensity contribution of slow mode A_s keeps constant at about 30 %, which is half of the contribution of the fast mode A_f dominated by macrocounterions. Therefore, the fast mode dominates over the slow mode for (PATP_ATRP)-MPC90%. However, for ordinary polyelectrolytes without added salt, slow mode dominates over the fast mode with $A_s \approx 60$ %.[4, 31] Therefore, the existence of macrocounterions results in more significant slow mode relaxation of polyelectrolytes. Further study on dynamic light scattering of polycations with macrocounterions on length scales of contour length of

Polymer Chemistry Accepted Manuscript

PATP-MPC90% and PATP-CPC45% are still under investigation.

Table 3. Diffusion coefficients of 2 mmol/L MPC, (PATP_ATRP)-OH in 10 mmol/L NaCl, (PATP_ATRP)-OH and (PATP_ATRP)-MPC90% .

Sample	**D / 10^{-7} cm^2 s^{-1}**	
MPC	11.5	
(PATP_ATRP)-OH in NaCl	3.19	
	D_f / 10^{-7} cm^2 s^{-1}	**D_s / 10^{-7} cm^2 s^{-1}**
(PATP_ATRP)-OH	37.0	2.58
(PATP_ATRP)-MPC90%	6.84	0.437

Conclusion

The present work is analyzed on the basis of the scaling theory, concerning the effective charge density, the static parameters and the dynamics of polycations with macrocounterions on various length scales. It is found that on length scale of contour length of polycations, a critical concentration (c^*_{mc}) exists. When concentration is below c^*_{mc}, the role of macrocounterions can be ignored; while above c^*_{mc}, macrocounterions dominate the relaxation of polycations and prevent entanglement of polycations. On length scale of electrostatic blobs, macrocounterions lead to significantly delayed bimodal diffusive relaxation and fast mode relaxation becomes dominant. Since no independent relaxation of macrocounterions has been observed, it is supposed that the fast mode relaxation is the coupled relaxation of polycations and macrocounterions. Moreover, macrocounterions can't serve as brushes condensed on the polycations until their molar fraction is above the effective charge density of polyelectrolytes. Polycations with macrocounterions may offer great chance to further

Polymer Chemistry Accepted Manuscript

explore the characteristics of polyelectrolyte relaxation, whereas many issues still require further investigation.

Acknowledgment

This work was supported by National Nature Science Foundation of China (No. 51473145) and the Fundamental Research Funds for the Central Universities (No. 2013QNA4048). The authors are grateful for the discussion with Professor Ralph Colby and Doctor Quan Chen of The Pennsylvania State University.

References

1. A. Deshkovski, S. Obukhov and M. Rubinstein, *Phys. Rev. Lett.*, 2001, **86**, 2341-2344.
2. M. Muthukumar, *J. Chem. Phys.*, 2004, **120**, 9343-9350.
3. H. Schiessel and P. Pincus, *Macromolecules*, 1998, **31**, 7953-7959.
4. H. Matsuoka, Y. Ogura and H. Yamaoka, *J. Chem. Phys.*, 1998, **109**, 6125-6132.
5. R. W. Chang and A. Yethiraj, *Journal of Chemical Physics*, 2002, **116**, 5284-5298.
6. M. Rubinstein and G. A. Papoian, *Soft Matter*, 2012, **8**, 9265-9267.
7. T. E. Angelini, L. K. Sanders, H. J. Liang, W. Wriggers, J. X. Tang and G. C. L. Wong, *J. Phys:Cond. Matter*, 2005, **17**, S1123-S1135.
8. M. Kanduc, A. Naji and R. Podgornik, *J. Chem. Phys.*, 2010, **132**.
9. G. Decher, J. D. Hong and J. Schmitt, *Thin Solid Films*, 1992, **210**, 831-835.
10. Q. Zhao, Q. F. F. An, Y. L. Ji, J. W. Qian and C. J. Gao, *J. Membr. Sci.*, 2011, **379**, 19-45.
11. J. P. Gong, Y. Katsuyama, T. Kurokawa and Y. Osada, *Adv. Mater.*, 2003, **15**, 1155-+.
12. A. V. Dobrynin, R. H. Colby and M. Rubinstein, *J. Polym. Sci. Part B:Polym. Phys.*, 2004, **42**, 3513-3538.
13. G. S. Georgiev, E. B. Karnenska, E. D. Vassileva, I. P. Kamenova, V. T. Georgieva, S. B. Iliev and I. A. Ivanov, *Biomacromolecules*, 2006, **7**, 1329-1334.
14. Y. B. Zhang, J. F. Douglas, B. D. Ermi and E. J. Amis, *J. Chem. Phys.*, 2001, **114**, 3299-3313.

Polymer Chemistry Accepted Manuscript

15. S. K. Filippov, T. A. P. Seery, J. Kriz, M. Hruby, P. Cernoch, O. Sedlacek, P. Kadlec, J. Panek and P. Stepanek, *Polym. Int.*, 2013, **62**, 1271-1276.
16. A. Mehrdad, M. T. Taghizadeh and R. Moladoust, *J. Solution. Chem.*, 2011, **40**, 832-842.
17. M. Spitzer, E. Sabadini and W. Loh, *J. Phys. Chem. B*, 2002, **106**, 12448-12452.
18. J.-H. H. Wang and R. H. Colby, *Soft Matter*, 2013, **9**, 10275-10286.
19. W. Wang, W. Liu, G. J. Tudryn, R. H. Colby and K. I. Winey, *Macromolecules*, 2010, **43**, 4223-4229.
20. J. Bodycomb and M. Hara, *Macromolecules*, 1995, **28**, 8190-8197.
21. A. V. Dobrynin, R. H. Colby and M. Rubinstein, *Macromolecules*, 1995, **28**, 1859-1871.
22. R. H. Colby, *Rheol. Acta*, 2010, **49**, 425-442.
23. S. Dou and R. H. Colby, *J. Polym. Sci. Part B:Polym. Phys.*, 2006, **44**, 2001-2013.
24. R. M. C. R. H., *Polymer Physics*, Oxford University Press, USA, 2003.
25. S. Namba, Y. Tsukahara, K. Kaeriyama, K. Okamoto and M. Takahashi, *Polymer*, 2000, **41**, 5165-5171.
26. S. Desvergne, V. Heroguez, Y. Gnanou and R. Borsali, *Macromolecules*, 2005, **38**, 2400-2409.
27. A. Papagiannopoulos, C. M. Fernyhough and T. A. Waigh, *J. Chem. Phys.*, 2005, **123**.
28. A. Papagiannopoulos, C. M. Fernyhough, T. A. Waigh and A. Radulescu, *Macromol. Chem. Phys.*, 2008, **209**, 2475-2486.
29. A. Papagiannopoulos, T. A. Waigh, T. Hardingham and M. Heinrich, *Biomacromolecules*, 2006, **7**, 2162-2172.
30. F Bordi, C Cametti, R H Colby, *J. Phys.: Condens. Matter.*, 2004, 16, 1423–1463.
31. K. J. Zhou, J. F. Li, Y. J. Lu, G. Z. Zhang, Z. W. Xie and C. Wu, *Macromolecules*, 2009, **42**, 7146-7154.

Polymer Chemistry Accepted Manuscript

Table of Contents

Rheological Behavior and Molecular Relaxation of Polycations with Macrocounterions in Aqueous Solutions

Yilan Ye [a, b], Shangguan Yonggang [*, a], Qiang Zheng [*, a]

[a] *MOE Key Laboratory of Macromolecular Synthesis and Functionalization, Department of Polymer Science and Engineering, Zhejiang University, Hangzhou 310027, China.*

[b] *Department of Materials Science and Engineering, The Pennsylvania State University, University Park, Pennsylvania 16802.*

* *Corresponding Authors. Email address: shangguan@zju.edu.cn (Yonggang Shangguan), zhengqiang@zju.edu.cn (Qiang Zheng). Tel: +86 57187953075.*

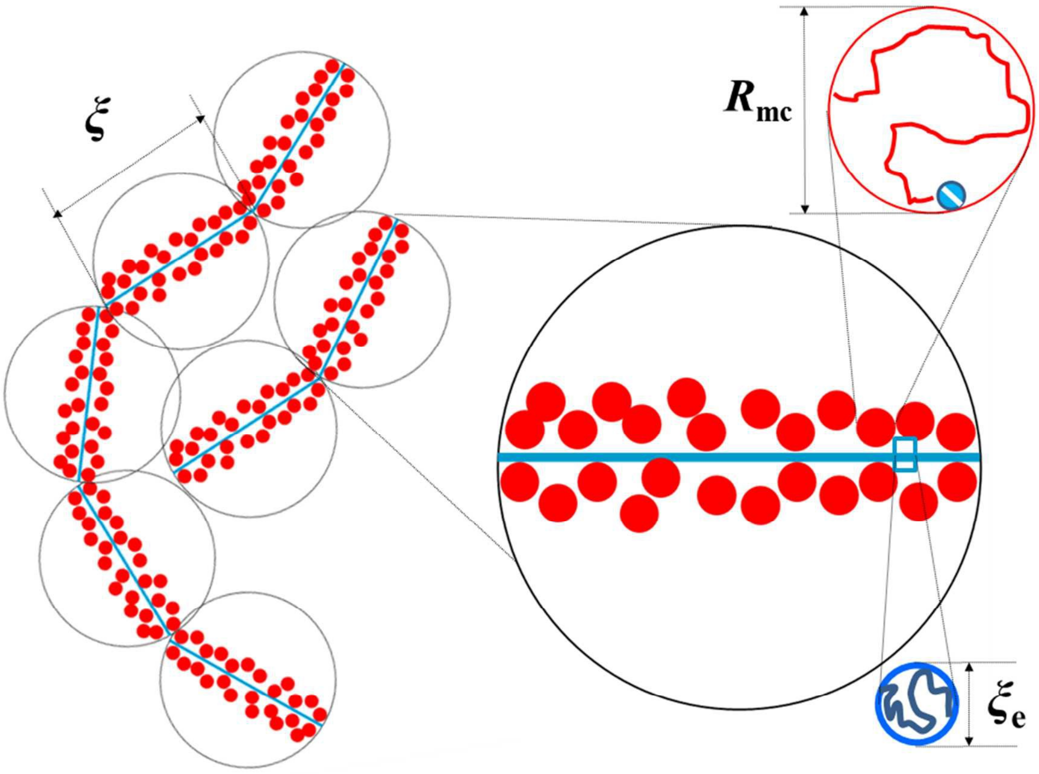

Polymer Chemistry Accepted Manuscript